Available online at www.sciencedirect.com
ScienceDirect
Medical Laser Application 22 (2007) 95–104
Medical Laser Application
www.elsevier.de/mla

Optical properties of human stomach mucosa in the spectral range from 400 to 2000 nm: Prognosis for gastroenterology

Alexey N. Bashkatov[a,*], Elina A. Genina[a], Vyacheslav I. Kochubey[a], Anna A. Gavrilova[a], Sergey V. Kapralov[b], Veniamin A. Grishaev[b], Valery V. Tuchin[b]

[a]*Research-Educational Institute of Optics and Biophotonics, Saratov State University, 83, Astrakhanskaya str., Saratov, 410012, Russia*
[b]*Department of Hospital Surgery of Saratov State Medical University, 112, B. Kazach'ya str., Saratov, 410012, Russia*

Received 12 June 2007; accepted 2 July 2007

Abstract

The optical properties of human stomach wall mucosa were measured in the wavelength range 400–2000 nm.The measurements were carried out using the commercially available spectrophotometer CARY-2415 with an integrating sphere. The combined method based on inverse adding-doubling and inverse Monte Carlo techniques was used to determine the absorption and scattering coefficients and anisotropy factor from the measurements.

Keywords: Optical properties; Absorption coefficient; Scattering coefficient; Anisotropy factor; Integrating sphere spectroscopy; Mucous tissue; Stomach; In vitro

Introduction

Recent technological advancements in the photonics industry have real progress toward the development of clinical functional imaging, surgical and therapeutic systems. Development of the optical methods in modern medicine in the areas of diagnostics, surgery and therapy has stimulated the investigation of optical properties of human tissues, since the efficacy of optical probing of the tissues depends on the photon propagation and fluence rate distribution within irradiated tissues. Examples of diagnostic use are the following: the monitoring of blood oxygenation and tissue metabolism [1,2], detection of stomach malignancies [3], and various recently suggested techniques for optical imaging [4,5]. Therapeutic usage mostly includes applications in laser surgery [6] and photodynamic therapy [7–9]. For these applications, the knowledge of tissue optical properties is of great importance to the interpretation and quantification of the diagnostic data, and to the prediction of light distribution and absorbed energy for therapeutic and surgical use. Numerous investigations related to determination of tissue optical properties are available in literature, however the optical properties of many tissues have not been studied in a wide wavelength range.

The goal of this paper is to measure optical properties (namely, absorption coefficient, scattering coefficient and anisotropy factor) of human stomach wall mucosa in the wavelength range from 400 to 2000 nm.

*Corresponding author. Tel.: +7 (845-2) 51 46 93; fax: +7 (845-2) 27 85 29.
E-mail address: a.n.bashkatov@mail.ru (A.N. Bashkatov).

1615-1615/$ - see front matter © 2007 Elsevier GmbH. All rights reserved.
doi:10.1016/j.mla.2007.07.003

Materials and methods

The measurements were carried out *in vitro* with fifteen human stomach wall mucosa samples, which were obtained from elective surgery. All samples were kept in saline at temperature about 5 °C until spectroscopic measurements. The samples were measured during 2–4 h after biopsy. All the samples have an area about 500–600 mm^2. For mechanical support, the tissue samples have been sandwiched between two glass slides. The thickness of each sample was measured with a micrometer in several points over the sample surface and averaged. Precision of the single measurement was ± 50 μm. Thickness of the samples varied from 0.95 ± 0.21 to 3.0 ± 0.08 mm.

The total (T_t) and diffuse (T_d) transmittance (equal to T_t minus the small angle portion of transmission within an angular aperture of 5.3 deg) and diffuse reflectance (R_d) measurements were performed in the 400–2000 nm wavelength range using the commercially available CARY-2415 (''Varian'', Australia) spectrophotometer with an integrating sphere. Inner diameter of the sphere is 100 mm, size of the entrance port is 20×20 mm and diameter of the exit port is 16 mm. As a light source, a halogen lamp with filtering of the radiation in the studied spectral range is used in the measurements. The diameter of incident light beam on the tissue sample is 3 mm. Scan rate is 2 nm/sec. The measurements were carried out at room temperature about 20 °C. For the measurement of T_t the exit port is closed with a certified white diffusive reflecting standard. T_d is measured after the standard was removed, so that nonscattered and scattered transmitted light leaves the sphere within an angle of 5.3 deg. Diffuse reflectance R_d is measured relative to the standard, first diffuse reflectance spectrum of standard is measured and then standard is replaced by the sample and its diffuse reflectance is measured. To avoid interference of Fresnel's reflectance from a sample surface with the diffuse reflectance, it was provided that specular beam leaves the integrating sphere through the open port.

For processing the experimental data and determination of the optical properties of tissue, the combined inverse method has been used. This method includes inverse adding-doubling (IAD) method developed by Prahl *et al* [10] and inverse Monte Carlo simulations. The IAD method is widely used in tissue optics for processing the experimental data of spectrophotometry with integrating spheres [10–16]. This method allows to determine the absorption (μ_a) and the reduced scattering coefficients $\left(\mu_s' = \mu_s(1-g)\right)$ of a tissue from the measured values of the total transmittance and the diffuse reflectance. Here μ_s is the scattering coefficient, and g is the anisotropy factor of the scattering. In these calculations the anisotropy factor has been fixed as 0.9, since this value is typical for the tissue in the visible and NIR spectral ranges [17]. The main advantage of the IAD method in comparison with many other methods of solution of the radiative transfer equation is connected with its validity for the arbitrary ratio of the absorption and scattering coefficients [10]. This property of the IAD method becomes essentially important in the case of determination of the optical properties of tissues within the strong absorption bands, when the values of the absorption and scattering coefficients become comparable. Other methods, for example, diffusion approximation [18] or Kubelka-Munk method [19], for their applicability require a fulfillment of the condition $\mu_a/\mu_s \ll 1$. The inverse Monte Carlo technique [20] can also be used for arbitrary ratio of μ_a and μ_s, but requires very extensive calculations. The main limitation of IAD method is connected with the possible loss of scattering radiation through lateral sides of a sample at calculations [21]. Loss of light through the sides of the sample and sample holder may erroneously increase the calculated value of the absorption coefficient. These losses depend on the physical size and geometry of the sample, i.e., the losses existing in the case, when the sizes of a sample do not exceed significantly the diameter of the incident beam. The size of the exit and the entrance ports of the integrating sphere are also important for errorless measurements of the total transmittance and the diffuse reflectance [21]. The tissue sample should completely cover the port in the integrating sphere, and the distance from the edge of irradiating beam on the sample to the edge of the port should be much larger than the lateral light propagation distance, which is determined as $1/\left(\mu_a + \mu_s'\right)$. If not so, light will be lost out from the sides of the sample and the loss will be attributed to absorption, and so the absorption coefficient will be overestimated. These requirements have been met in our experiments, since maximal size of the sphere port does not exceed 20 mm, while the minimal size of the mucosa samples is 20 mm. In addition, using the absorption and the reduced scattering coefficients of the tissue samples presented below, in the next section, we calculated the lateral light propagation distance. For the tissue the maximal lateral light propagation distance is equal to 1.19 mm for the wavelength 1280 nm. Taking into account the diameter of the incident beam (3 mm), minimal size of a tissue sample has to be larger than 4.5 mm that was satisfied for each tissue sample under study. It is seen, that the lateral light propagation distance is smaller than the distance from the edge of the irradiating beam on the sample to the sample port edge. Besides, Pickering *et al* [21] have reported that area of tissue sample has to be smaller than the area of the inner surface of the integrating sphere. This requirement has also been met in our experiments, since the area of the inner surface of integrating sphere used in the measurements was 314.16 cm^2, while the area of the

tissue samples does not exceed 6.0 cm^2. Fig. 1 shows the geometry and parameters of the measurements in the transmittance and reflectance modes, respectively.

Calculation of the tissue absorption and reduced scattering coefficients by the IAD method was performed for each wavelength. The algorithm consists of the following steps: (a) the estimation of a set of the optical parameters; (b) the calculation of the reflectance and transmittance with the adding-doubling iterative method; (c) the comparison of the calculated with the measured values of the diffuse reflectance and the total transmittance; (d) iteration of the above steps until a match (within the specified acceptance margin) is reached. With this iterative process the set of optical properties that yields the closest match to the measured values of reflectance and transmittance are taken as the optical properties of the tissue.

Based on the obtained values of the tissue absorption and reduced scattering coefficients the inverse Monte Carlo calculations have been performed. The inverse method includes direct problem, i.e. Monte Carlo simulation, which takes into account the geometric and optical conditions (sample geometry, sphere parameters, refractive index mismatch, etc.), and solution to inverse problem, i.e. minimization of target function by an iteration method. In this study, we used Monte Carlo algorithm developed by L. Wang and S. Jacques [22]. The stochastic numerical MC method is widely used to model optical radiation propagation in complex randomly inhomogeneous highly scattering and absorbing media such as biological tissues [17,20,23]. Basic MC modeling of an individual photon packets trajectory consists of the sequence of the elementary simulations [22]: photon pathlength generation, scattering and absorption events, reflection or/and refraction on the medium boundaries. The specular reflection from the air-glass-tissue interface is taken into account in the simulations. At the scattering site a new photon packet direction is determined according to the Henyey–Greenstein scattering phase function:

$$f_{\mathrm{HG}}(\theta) = \frac{1}{4\pi}\frac{1-g^2}{(1+g^2-2g\cos\theta)^{3/2}},$$

where θ is the polar scattering angle. The distribution over the azimuthal scattering angle was assumed as uniform.

Usually the inverse Monte Carlo technique requires very extensive calculations since all tissue optical parameters (absorption and scattering coefficients and anisotropy factor) are unknown. To avoid the lengthy calculations in this study we used values of absorption coefficients obtained from calculations performed by IAD method. Scattering coefficients have been calculated from the relation $\mu_s = \mu_s'/(1-g)$, where μ_s' values have been obtained from IAD calculations. For determination of the tissue anisotropy factor g minimization of the following target function has been

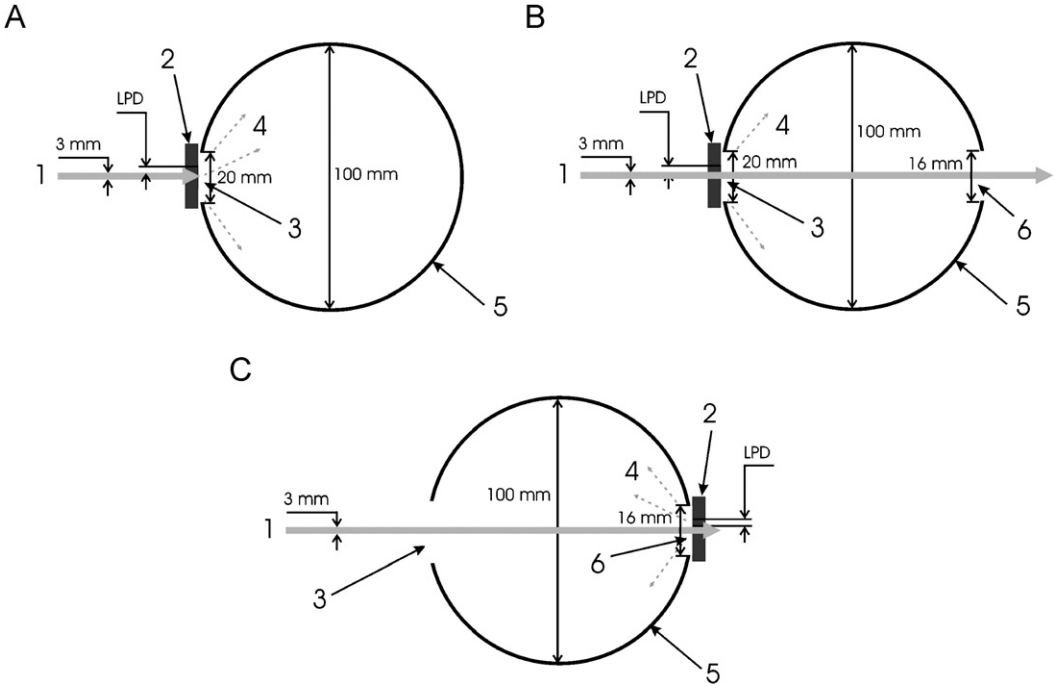

Fig. 1. The geometry of the measurements in (A) total transmittance mode, (B) diffuse transmittance mode, (C) reflectance mode. 1–the incident beam (diameter 3 mm); 2–the tissue sample; 3–the entrance port (square 20 × 20 mm); 4–the transmitted (or diffuse reflected) radiation; 5–the integrating sphere (inner diameter is 100 mm); 6–the exit port (diameter 16 mm). LPD–the maximal value of lateral light propagation distance.

performed

$$F(g) = \left(R_d^{\exp} - R_d^{\text{calc}}(\mu_a, \mu_s, g)\right)^2 + \left(T_d^{\exp} - T_d^{\text{calc}}(\mu_a, \mu_s, g)\right)^2 + \left(T_t^{\exp} - T_t^{\text{calc}}(\mu_a, \mu_s, g)\right)^2,$$

with the boundary condition $0 \leqslant g \leqslant 0.98$. To minimize the target function the Levenberg-Marquardt nonlinear least-squares-fitting algorithm described in detail by Press *et al* [24] has been used. Iteration procedure repeats until experimental and calculated data are matched within a defined error limit (<0.5%). Here $R_d^{\exp}$, $T_d^{\exp}$, $T_t^{\exp}$, R_d^{calc}, T_d^{calc}, T_t^{calc} are measured and calculated values of diffuse reflectance and diffuse and total transmittance, respectively.

Results and discussion

Fifteen human stomach wall mucosa samples obtained from elective surgery were used for the in vitro measurements. Fig. 2 shows the reflectance and transmittance spectra of the tissue sample measured in the spectral range from 400 to 2000 nm. Thickness of the sample is 1.0 ± 0.1 mm. In the visible spectral range, the form of the presented spectra is defined by the absorption bands of blood of the mucous tissue and the spectral dependence of scattering coefficient of the tissue. In the infrared spectral range, absorption bands of water of interstitial matrix define the form of the spectra.

Figs. 3 and 4 show the measured optical properties of the mucous tissue calculated by IAD method on the basis of measured values of the total transmittance and the diffuse reflectance. Fig. 3 presents the wavelength dependence of the tissue absorption coefficient in the spectral range from 400 to 2000 nm. The vertical lines correspond to the values of standard deviation (*SD*), which is determined as:

$$SD = \sqrt{\sum_{i=1}^{n} \left(\bar{\mu}_a - \mu_{a\,i}\right)^2 / n(n-1)},$$

where $n = 15$ is number of the measured tissue samples, μ_{ai} is the absorption coefficient of each sample, and $\bar{\mu}_a$ is the mean value of the absorption coefficient for each wavelength, which is calculated as

$$\sum_{i=1}^{n} \mu_{a\,i}/n.$$

In the spectrum, absorption bands of blood hemoglobin (420 and 550 nm [25]) and water (1450 and 1940 nm [26,27]) are clearly visible. The absorption bands of water located at 980, 1189 and 1787 nm [26,27] are considerably less observed.

Fig. 4 presents the spectral dependence of the reduced scattering coefficient of the mucous tissue. This dependence was obtained by averaging of the spectra of the reduced scattering coefficient of the fifteen samples of the mucous tissue. It is clearly seen that, with increase of wavelength, the reduced scattering coefficient decreases smoothly, which corresponds to the general spectral behavior of the scattering characteristics of biological tissues [28–30]. However, in the range of the strong absorption bands of water (1450 and 1940 nm), the shape of the scattering spectrum deviates from a monotonic dependence. At the same time, in the range

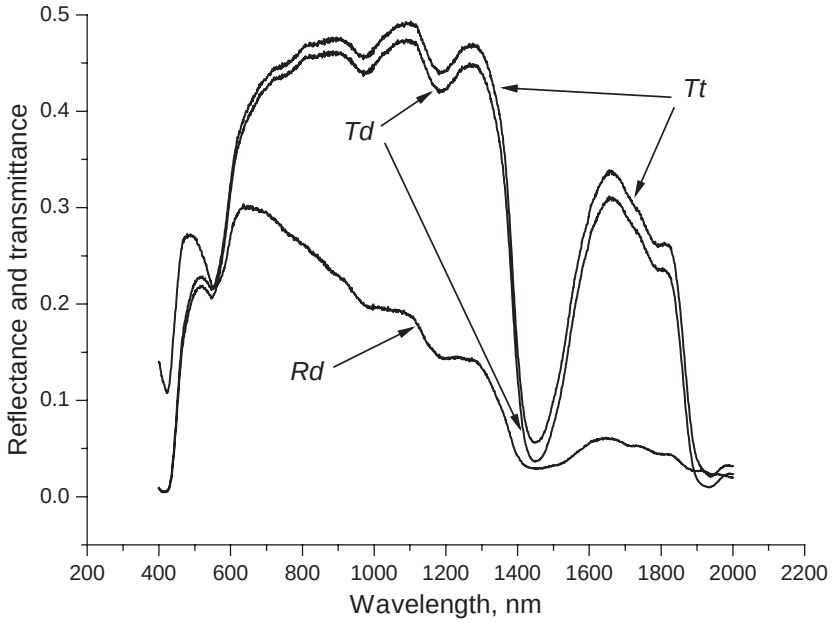

Fig. 2. The diffuse reflectance and total and diffuse transmittance spectra of human stomach wall mucosa sample. Thickness of the sample is 1.0 ± 0.1 mm.

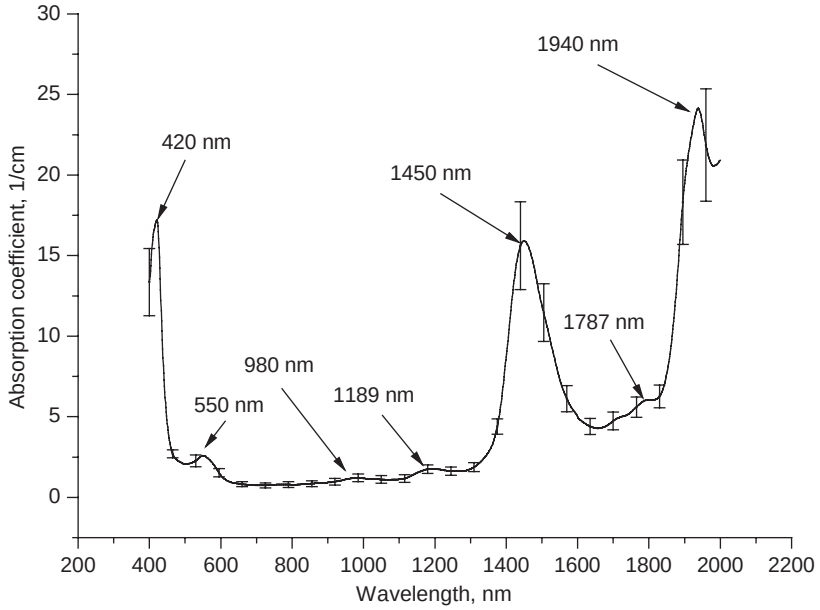

Fig. 3. The wavelength dependence of the absorption coefficient of human stomach wall mucosa. The vertical lines show the standard deviation values.

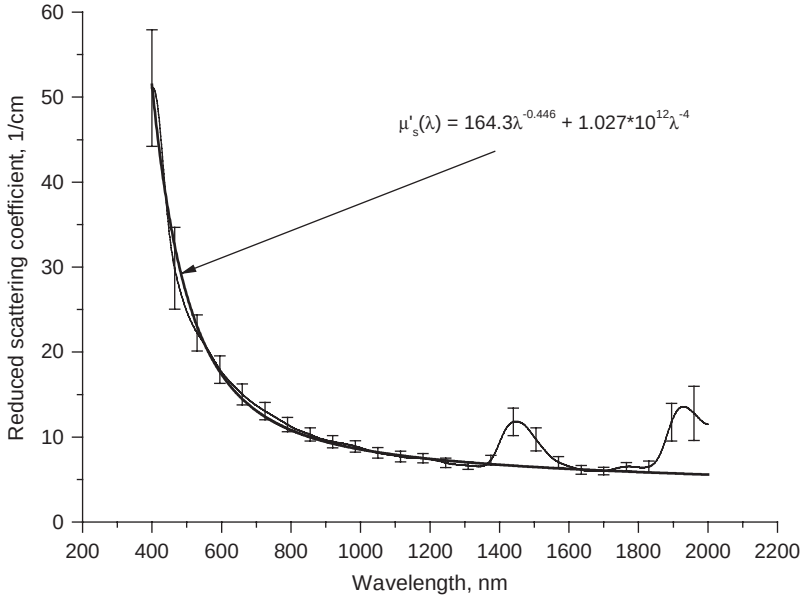

Fig. 4. The spectral dependence of the reduced scattering coefficient of human stomach wall mucosa and its approximation by power law. The vertical lines show the standard deviation values.

of the water absorption bands with maximums at 980, 1189 and 1787 nm the effect is not observed.

In the spectral range 600–1500 nm for many tissues the reduced scattering coefficient decreases with the wavelength in accordance with a power law $\mu_s'(\lambda) = a\lambda^{-w}$ [28–30]. The wavelength exponent w characterizes the mean size of the tissue scatterers and defines spectral behavior of the reduced scattering coefficient. Fig. 4 shows approximation of the wavelength dependence of the reduced scattering coefficient by the power law $\mu_s'(\lambda) = 164.3\lambda^{-0.446} + 1.027 \times 10^{12}\lambda^{-4}$, where λ is wavelength, nm. In the Fig. 4 it is seen, that in the spectral ranges from 400 to 1350 nm and from 1600 to 1800 nm this power law well approximates the experimental data, in contrast to the data in the spectral range 1350–1600 nm and 1800–2000 nm, which corresponds to strong water absorption bands.

Typically, the value of the wavelength exponent obtained for aorta, skin, eye sclera, *dura mater* etc are in the range from 1 to 2, which is defined by the major

scatterer type [29–34]. Doornbos *et al* [31] and Vargas *et al* [33] reported the wavelength exponent as 1.11 and 1.12, respectively, in the spectral range 500–1200 nm. Bashkatov *et al* [11] approximating the data of Simpson *et al* [35] in the spectral range 620–1000 nm and Chan *et al* [36] in the spectral range 400–1800 nm found w equal to 1.4 and 1.13, respectively. However, for data of Troy *et al* [16] in the spectral range 1000–1250 nm they obtained $w = 0.7$. Thus, it can be seen, that the wavelength exponent values obtained from different spectral ranges are various. In assumption that in the visible spectral range (400–700 nm) refractive indices of tissue scatterers and interstitial fluid are 1.45 and 1.36 [17,29,30], respectively, the corresponding estimated mean size of the scatterers are in the ranges from 0.2 to 0.5 μm. At the same time, it should be noted, that the values indicate the mean size of scatterers only. In contrast to this, we obtained a very low value of the wavelength exponent, i.e. $w = 0.446$, in the spectral range 1350–2000 nm. This value is close to the value of the wavelength exponent $w = 0.23$ in the spectral range 900–1350 nm following from data of Du *et al* [37] and $w = 0.22$ [11]. This value is also close to the predicted one by Graaff *et al* [38] for the mixture of large spherical particles, i.e. $\mu_s' \sim \lambda^{-0.37}$. One of the possible reasons for these large differences is the complex multi-component structure of human tissues. The presence of large so-called Mie scatterers produces a weak wavelength dependence of the scattering coefficient in the IR spectral range. However, in the spectral range 400–1000 nm the wavelength dependence of the reduced scattering coefficient could not be described by the power law with $w = 0.446$. In this spectral range the reduced scattering coefficient decreases abruptly and the effect of the decreasing of the reduced scattering coefficient can be explained by contribution of small, so-called Rayleigh scatterers, i.e. collagen and elastin fibrils. The Rayleigh scattering can be represented as $\mu_s'(\text{Rayleigh}) = b\lambda^{-4}$, where the factor b varies only with the magnitude of Rayleigh scattering. The measured reduced scattering coefficient spectrum, which is a combination of Mie and Rayleigh scattering spectra, has been fitted by:

$$\mu_s'(\text{measured}) = \mu_s'(\text{Mie}) + \mu_s'(\text{Rayleigh}) = 164.3\lambda^{-0.446} + b\lambda^{-4},$$

and the factor b has been estimated from the fitting as 1.027×10^{12}. In Fig. 4 is seen, that the combination of the wavelength dependencies of the Rayleigh and Mie scattering very well describes the measured wavelength dependence of the reduced scattering coefficient.

The fraction f_{Rayleigh} of the total reduced scattering that is due to Rayleigh scattering by collagen fibrils can be calculated as

$$f_{\text{Rayleigh}} = \frac{1.027 \times 10^{12}\lambda^{-4}}{164.3\lambda^{-0.446} + 1.027 \times 10^{12}\lambda^{-4}}.$$

Result of the calculations is presented in Fig. 5. It is seen, that in the visible spectral range the Rayleigh scattering is dominant, but with the increase of the wavelength the contribution of the Rayleigh scattering decreases sharply and in the NIR the contribution is insignificant.

The depth penetration of light into a biological tissue is an important parameter for the correct determination of the irradiation dose in photothermal and

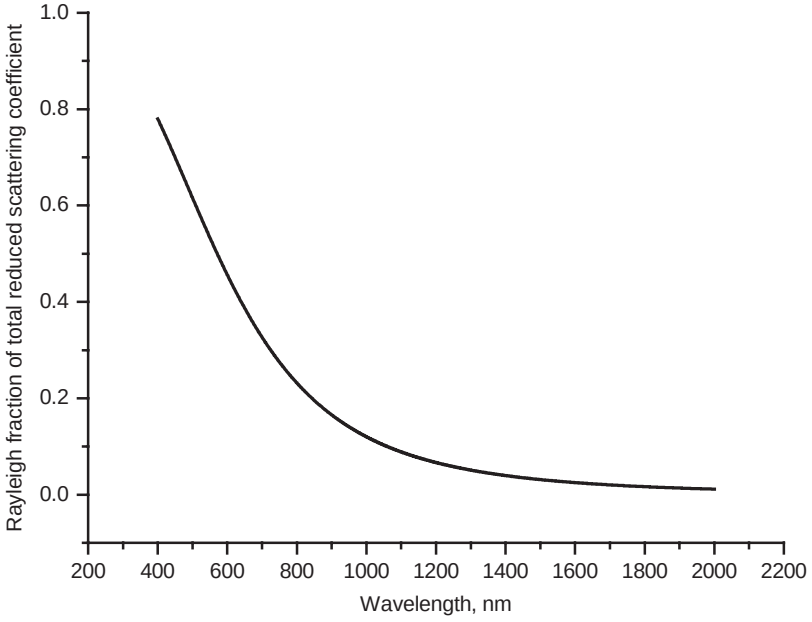

Fig. 5. Fraction of total reduced scattering attributed to Rayleigh scattering.

photodynamic therapy of various diseases [17]. Estimation of the light penetration depth δ can be performed with the relation:

$$\delta = 1 \Big/ \sqrt{3\mu_a(\mu_a + \mu_s')}.$$

Calculation of the optical penetration depth has been performed with the absorption and reduced scattering coefficient values presented in Figs. 3 and 4 and the result presented in Fig. 6. In Fig. 6, it is seen that maximal penetration depth 1.9 mm is observed at the wavelength 815 nm.

The effect of deviation of wavelength dependence of the reduced scattering coefficient from the power law dependence, i.e. the increase of the reduced scattering coefficients in the spectral ranges 1350–1600 nm and 1800–2000 nm with peaks corresponding to the absorption bands, can be connected with the increase of imaginary part of complex refractive index of the tissue scatterers and interstitial fluid in the range of the absorption bands. The increase of the imaginary part of the refractive indices produces significant decrease of the anisotropy factor g, which, along with the scattering coefficient μ_s of a tissue, forms the tissue reduced scattering coefficient. In [23] and [37] it was experimentally shown that in the range of water absorption bands, with maximum at 1450 and 1930 nm, significant decrease of the anisotropy factor is observed that produces the increase of the reduced scattering coefficient and appearance of bands in its spectrum. Note, that the degree of decrease of the anisotropy factor in the range of absorption bands is proportional to intensity of the absorption bands. This was confirmed by Fu and Sun [39] and Sun *et al* [40] who developed theory and computer model of light scattering on scattering particles immersed in an absorbing host medium. In the model these authors demonstrated that for large scatterers immersed in an absorbing medium decreasing of scattering coefficient and significant decreasing anisotropy factor (up to negative values) could be observed.

In Fig. 3 one can see, that in the spectral range 600–1350 nm the absorption of the mucous tissue is small. Hence, the scattering properties of the tissue are defined only by the real part of complex refractive index and the reduced scattering coefficient decreases rather monotonically with the wavelength (see Fig. 4). In the spectral range 1350–2000 nm the absorption bands of water are observed (see Fig. 3). The presence of the strong absorption bands leads to the fact that the scattering properties are formed not only under influence of the real, but also the imaginary part of a complex refractive index of the scattering centers and interstitial fluid, that produces increasing of the reduced scattering coefficient in the given spectral region with rather strong peaks in the range of the absorption bands. Insignificant shift of maxima of the peaks in spectrum of the reduced scattering coefficient in comparison with maxima of the absorption bands (see Figs. 3 and 4) can be explained by anomalous light dispersion, since within an absorption band the real part of refractive index corresponding to the short-wavelength wing of the absorption band goes down, and at the long-wavelength wing it goes up.

Using the inverse Monte Carlo method and values of absorption and reduced scattering coefficients calculated by inverse adding-doubling method the wavelength dependence of scattering coefficient (see Fig. 7) and

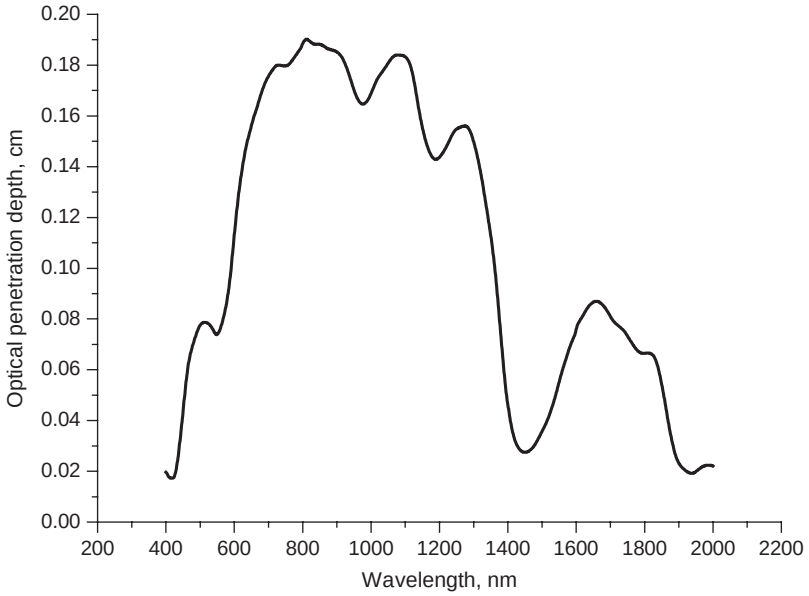

Fig. 6. The optical penetration depth δ of light into stomach mucosa over the wavelength range from 400 to 2000 nm.

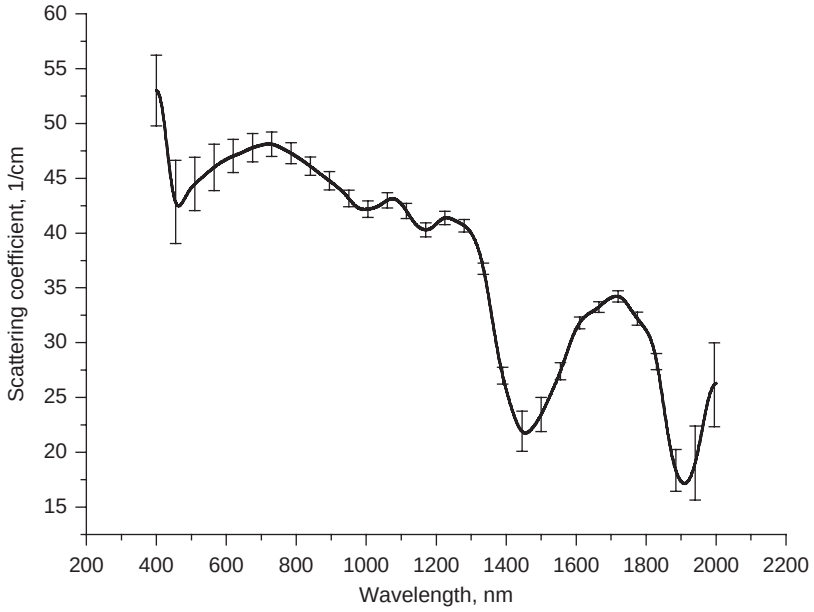

Fig. 7. The spectral dependence of the scattering coefficient of human stomach wall mucosa. The vertical lines show the standard deviation values.

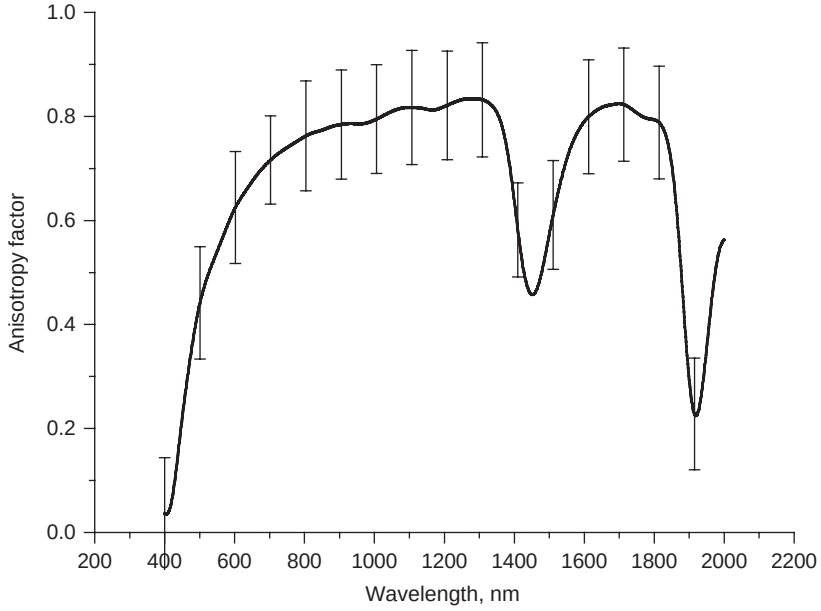

Fig. 8. The spectral dependence of the anisotropy factor of human stomach wall mucosa. The vertical lines show the standard deviation values.

anisotropy factor (see Fig. 8) of human stomach wall mucosa have been calculated. From Fig. 7 it is clearly seen that in the spectral ranges corresponding to the tissue absorption bands the scattering coefficient is significantly decreased and depth of the decrease is correlated with intensity of the absorption bands. Fig. 8 shows the spectral dependence of anisotropy factor of human stomach wall mucosa. In Fig. 8 is seen that anisotropy factor significantly decreases in the spectral ranges correspond to the tissue absorption bands. Such behavior agrees with the experimental data presented in [23] and [37] and theoretical calculations presented in [39] and [40].

Conclusion

The absorption and the scattering coefficients, and the anisotropy factor of the human stomach wall mucosa in vitro have been determined over the wavelength range 400–2000 nm using the integrating sphere technique, and

the combined method based on the inverse adding-doubling and Monte Carlo methods. In this spectral range the absorption bands of hemoglobin at 420 and 550 nm and water at 980, 1189, 1450, 1787, and 1940 nm are observed. For the human stomach wall mucosa tissue in the spectral range from 400 to 2000 nm, the wavelength dependence of the reduced scattering coefficient can be described as $\mu_s'(\lambda) = 164.3\lambda^{-0.446} + 1.027 \times 10^{12}\lambda^{-4}$. The presented results can be used for the development and optimization of optical diagnostic, therapeutic and surgical systems and can be useful in tissue optics.

Acknowledgments

The research described in this publication has been made possible, in part, by grants PG05-006-2 and REC-006 of US Civilian Research and Development Foundation for the Independent States of the Former Soviet Union (CRDF) and the Russian Ministry of Science and Education, grant of the Russian Federal Agency of Education Russian Federation 1.4.06, and grant of RFBR No. 06-02-16740-a. The authors thank Dr. S.V. Eremina (Department of English and Intercultural Communication of Saratov State University) for the help in manuscript translation to English.

Zusammenfassung

Optische Eigenschaften der humanen Magenschleimhaut im Spektralbereich von 400 bis 2000 nm: Prognose für die Gastroenterologie.

Die optischen Eigenschaften humaner Magenschleimhaut wurden für den Wellenlängenbereich von 400–2000 nm bestimmt. Die Messungen wurden mit einem kommerziell erhältlichen Spektrophotometer (CARY-2415) und einer Ulbrichtkugel durchgeführt. Dabei wurde eine Kombination aus „*Inverse Adding-Doubling*-“ und inversen Monte Carlo-Techniken verwendet, um die Absorptions- und Streuquerschnitte sowie Anisotropiefaktoren aus den experimentellen Messungen zu bestimmen.

Schlüsselwörter: Optische Eigenschaften; Absorptionskoeffizient; Streukoeffizient; Anisotropiefaktor; Ulbrichtkugel; Schleimhautgewebe; Magen; In vitro

Resumen

Propiedades ópticas de la mucosa estomacal humana en el rango spectral de los 400 a los 2000 nm: pronóstico para la gastroenterología

Las propiedades ópticas de la mucosa del estómago humano fueron determinadas en longitudes de onda en el rango de 400–2000 nm.Las medidas fueron efectuadas mediante un espectrofotómetro CARY-2415, disponible comercialmente, con una esfera integradora. Con el fin de determinar los coeficientes de absorción y dispersión y el factor de anisotropía a partir de las mediciones, se utilizó una combinación del método IAD (*Inverse Adding-Doubling*) y la Simulación inversa de Monte Carlo.

Palabras clave: Propiedades ópticas; Coeficiente de absorción; Coeficiente de dispersión; Factor de anisotropía; Esfera integradora espectroscopía; Mucosa; Estómago; In vitro

References

[1] Friedland S, Benaron D, Parachikov I, Soetikno R. Measurement of mucosal capillary hemoglobin oxygen saturation in the colon by reflectance spectrophotometry. Gastrointest. Endosc. 2003;57(4):492–7.

[2] Friedland S, Soetikno R, Benaron D. Reflectance spectrophotometry for the assessment of mucosal perfusion in the gastrointestinal tract. Gastrointest. Endosc. Clinics of North America 2004;14:539–53.

[3] Orth K, Russ D, Steiner R, Beger HG. Fluorescence detection of small gastrointestinal tumours: principles, technique, first clinical experience. Langenbeck's Arch. Surg. 2000;385:488–94.

[4] Tearney GJ, Brezinski ME, Southern JF, Bouma BE, Boppart SA, Fujimoto JG. Optical biopsy in human gastrointestinal tissue using optical coherence tomography. Am. J. Gastroenterology 1997;92(10):1800–4.

[5] Thueler P, Charvet I, Bevilacqua F, Ghislain M, Ory G, Marquet P, Meda P, Vermeulen B, Depeursinge C. In vivo endoscopic tissue diagnostics based on spectroscopic absorption, scattering, and phase function properties. J. Biomed. Opt. 2003;8(3):495–503.

[6] Mathus-Vliegen EMH, Tytgat G N J. Nd-YAG laser photocoagulation in gastroenterology: its role in palliation of colorectal cancer. Lasers Med. Sci. 1986; 1:75–80.

[7] Krasner N, Chatlani PT, Barr H. Photodynamic therapy of tumours in gastroenterology – a review. Lasers Med. Sci. 1990;5:233–9.

[8] Maier A, Anegg U, Fell B, Tomaselli F, Sankin O, Prettenhofer U, Pinter H, Rehak P, Friehs GB, Smolle-Juttner FM. Effect of photodynamic therapy in a multimodal approach for advanced carcinoma of the gastroesophageal junction. Lasers Surg. Med. 2000;26: 461–6.

[9] Roche JVE, Whitehurst C, Watt P, Moore JV, Krasner N. Photodynamic therapy (PDT) of gastrointestinal tumours: a new light delivery system. Lasers Med. Sci. 1998;13:137–42.

[10] Prahl SA, van Gemert MJC, Welch AJ. Determining the optical properties of turbid media by using the adding-doubling method. Appl. Opt. 1993;32:559–68.

[11] Bashkatov AN, Genina EA, Kochubey VI, Tuchin VV. Optical properties of human skin, subcutaneous and mucous tissues in the wavelength range from 400 to 2000 nm. J. Phys. D: Appl. Phys. 2005;38:2543–55.

[12] Nemati B, Rylander III JG, Welch AJ. Optical properties of conjunctiva, sclera, and the ciliary body and their consequences for transscleral cyclophotocoagulation. Appl. Opt. 1996;35:3321–7.
[13] Beek JF, Blokland P, Posthumus P, Aalders M, Pickering JW, Sterenborg HJCM, van Gemert MJC. In vitro double-integrating-sphere optical properties of tissues between 630 and 1064 nm. Phys. Med. Biol. 1997;42: 2255–61.
[14] Bashkatov AN, Genina EA, Kochubey VI, Tuchin VV. Estimation of wavelength dependence of refractive index of collagen fibers of scleral tissue. Proc. SPIE 2000;4162:265–8.
[15] Sardar DK, Mayo ML, Glickman RD. Optical characterization of melanin. J. Biomed. Opt. 2001;6:404–11.
[16] Troy TL, Thennadil SN. Optical properties of human skin in the near infrared wavelength range of 1000 to 2200 nm. J. Biomed. Opt. 2001;6:167–76.
[17] Tuchin VV. Tissue Optics: Light Scattering Methods and Instruments for Medical Diagnosis. Bellingham: SPIE Press; 2000.
[18] Farrell TJ, Patterson MS, Wilson BC. A diffusion theory model of spatially resolved, steady-state diffuse reflectance for the noninvasive determination of tissue optical properties in vivo. Med. Phys. 1992;19:879–88.
[19] Vargas WE. Inversion methods from Kubelka-Munk analysis. J. Opt. A: Pure Appl. Opt. 2002;4:452–6.
[20] Yaroslavsky I V, Yaroslavsky AN, Goldbach T, Schwarzmaier H-J. Inverse hybrid technique for determining the optical properties of turbid media from integrating-sphere measurements. Appl. Opt. 1996;35:6797–809.
[21] Pickering JW, Prahl SA, van Wieringen N, Beek JF, Sterenborg HJCM, van Gemert MJC. Double-integrating-sphere system for measuring the optical properties of tissue. Appl. Opt. 1993;32:399–410.
[22] Wang L, Jacques SL, Zheng L. MCML – Monte Carlo modeling of light transport in multi-layered tissues. Computer Methods and Programs in Biomedicine 1995;47:131–46.
[23] Ritz J-P, Roggan A, Isbert C, Müller G, Buhr H, Germer C-T. Optical properties of native and coagulated porcine liver tissue between 400 and 2400 nm. Lasers Surg. Med. 2001;29:205–12.
[24] Press WH, Tuekolsky SA, Vettering WT, Flannery BP. Numerical Recipes in C: The Art of Scientific Computing. Cambridge: Cambridge University Press; 1992.
[25] Prahl S A. Optical absorption of hemoglobin. http://www.omlc.ogi.edu/spectra/, 1999.
[26] Palmer KF, Williams D. Optical properties of water in the near infrared. J. Opt. Soc. Am. 1974;64:1107–10.
[27] Kou L, Labrie D, Chylek P. Refractive indices of water and ice in the 0.65–2.5 μm spectral range. Appl. Opt. 1993;32:3531–40.
[28] Mourant JR, Fuselier T, Boyer J, Johnson TM, Bigio IJ. Predictions and measurements of scattering and absorption over broad wavelength ranges in tissue phantoms. Appl. Opt. 1997;36:949–57.
[29] Schmitt JM, Kumar G. Optical scattering properties of soft tissue: a discrete particle model. Appl. Opt. 1998;37: 2788–97.
[30] Wang RK. Modelling optical properties of soft tissue by fractal distribution of scatterers. J. Modern Opt. 2000; 47:103–20.
[31] Doornbos RMP, Lang R, Aalders MC, Cross FW, Sterenborg HJCM. The determination of in vivo human tissue optical properties and absolute chromophore concentrations using spatially resolved steady-state diffuse reflectance spectroscopy. Phys. Med. Biol. 1999;44: 967–81.
[32] Cilesiz IF, Welch AJ. Light dosimetry: effects of dehydration and thermal damage on the optical properties of the human aorta. Appl. Opt. 1993;32:477–4787.
[33] Vargas G, Chan EK, Barton JK, Rylander III HG, Welch AJ. Use of an agent to reduce scattering in skin. Lasers Surg. Med. 1999;24:133–41.
[34] Ghosh N, Mohanty SK, Majumder SK, Gupta PK. Measurement of optical transport properties of normal and malignant human breast tissue. Appl. Opt. 2001;40: 176–84.
[35] Simpson CR, Kohl M, Essenpreis M, Cope M. Near-infrared optical properties of *ex vivo* human skin and subcutaneous tissues measured using the Monte Carlo inversion technique. Phys. Med. Biol. 1998;43:2465–78.
[36] Chan EK, Sorg B, Protsenko D, O'Neil M, Motamedi M, Welch AJ. Effects of compression on soft tissue optical properties. IEEE J. Quantum Electronics 1996;2:943–50.
[37] Du Y, Hu XH, Cariveau M, Kalmus GW, Lu JQ. Optical properties of porcine skin dermis between 900 nm and 1500 nm. Phys. Med. Biol. 2001;46:167–81.
[38] Graaff R, Aarnoudse JG, Zijp JR, Sloot PMA, de Mul FFM, Greve J, Koelink MH. Reduced light-scattering properties for mixtures of spherical particles: a simple approximation derived from Mie calculations. Appl. Opt. 1992;31:1370–6.
[39] Fu Q, Sun W. Mie theory for light scattering by a spherical particle in an absorbing medium. Appl. Opt. 2001;40:1354–61.
[40] Sun W, Loeb N G, Lin B. Light scattering by an infinite circular cylinder immersed in an absorbing medium. Appl. Opt. 2005;44:2338–42.